大和大学　研究紀要　第７巻　理工学部編　2021年３月　pp.7～13

A Study on Tolerance Design of Parallel Link Robots Based on Mathematical Models

Nobuhiro Sugimura*

Prof., Dr., Faculty of Science and Engineering, Yamato University
2-5-1 Katayama-cho, Suita-shi, Osaka 564-0082, Japan

Abstract

Parallel link robots are now being applied to various assembling tasks for small products and components. One of the important issues for design of the parallel link robots is to improve their kinematic motion deviations due to the complex link structures. The kinematic motion deviations of the parallel link robots are deeply influenced by the geometric deviations of the components, such as joints and links. A systematic design method is required for specifying suitable geometric tolerances of the joints and the links, in order to improve the kinematic motion deviations of the parallel link robots. The objective of the paper is to establish a computer-aided design system for specifying a suitable set of the geometric tolerances of the components considering the trade-off between the requirements on the kinematic motion deviations and the ease of the manufacturing processes. A mathematical model is formulated to represent the standard deviations of the kinematic motions of the end effectors, based on the tolerance values of the joints and the links. A systematic method is proposed here, by applying an optimization method, to determine a suitable set of the tolerance values of all the joints and the links under the constraints on the kinematic motion deviations of the end effectors. The method is applied to some design problems of the geometric tolerances of the parallel link robots.

Keywords: Tolerance Design, Geometric Dimensioning and Tolerancing, Modeling, Kinematic Motion Deviations.

1. Introduction

Parallel link robots are now being applied to various assembling tasks and picking tasks for small products and components. One of the important issues for design of the parallel link robots is to improve their kinematic motion deviations due to the complex link structures. The kinematic motion deviations of the parallel link robots are deeply influenced by the geometric deviations of the components, such as joints and links.

Three-dimensional CAD/CAM/CAE (Computer Aided Design/Manufacturing/Engineering) systems are now being widely applied to design, analysis and manufacturing of machine products and components. One of the important issues to be considered in the applications of CAD/CAM/CAE systems is how to deal with the geometric tolerancing and the dimensional tolerancing in the three-dimensional product modeling systems. Some researches have been carried out to deal with the dimensional tolerances and the geometric tolerances, aimed at realizing statistical analysis and design methodologies for 3-dimensional machine products [1-8]. In the previous papers, a systematic method was proposed to determine a suitable set of the tolerance values of the guide-ways of the 5-axis machining centers under the constraints on the kinematic motion deviations of the feed motions, by applying mathematical models of the shape generation motions of the machine tools [9-12].

The objective of the paper is to propose a mathematical model for the CAD/CAE/CAM systems with the capability to analyze the kinematic motion deviations of the parallel link robots. The mathematical model represents the kinematic motion deviations of parallel link robots, on the basis of the dimensions and geometric tolerances of the components. The proposed model is applied to the systematic procedure which determine both the dimensional tolerances and the geometric tolerances of the joints and the links under the constraints on the kinematic motion deviations of parallel link robots.

2. Geometric Tolerances and Deviations of Features [7-9]

The geometric tolerances of the features specify the allowable areas named "tolerance zones," which constrain the position and orientation deviations of the associated features against the nominal features, as shown in Fig. 1 (a). The associated features and the nominal features mean the features of the manufactured products and the ideal features defined in the design phase, respectively. The geometric deviations of the associated features from the nominal features are represented by sets of parameters named "deviation parameters." For example, one position parameter w and two rotational parameters α and β are required to represent the geometric deviations of the associated plane features against the nominal plane features, for the case where the tolerance zone is given by the area between a pair of parallel planes. In the research, the followings are assumed for the ease of the modeling and the analysis of the geometric deviations.

(1) The deviation parameters δ_i representing the position and orientation deviations of the associated features follow the normal distribution $N(\mu_i, \sigma_i)$, and μ_i =0. Where, μ_i and σ_i are the mean values and the standard deviations, respectively.

(2) The manufacturing processes of the components are well controlled, and the proportion of the non-conforming components, which means the toleranced features exceed the tolerance zones, is as small as a value P_d called "Defective rate".

(3) Eq. (1) represents the relationships between the standard deviations σ_i of the deviation parameters of the tolerance features and the maximum values of the deviation parameters.

$$\sigma_i = \delta_{imax}/C_{Pd} \tag{1}$$

*大和大学理工学部

令和２年11月６日受理

where,

δ_{imax} : Maximum values of the deviation parameters δ_i, if the other deviation parameters are $\delta_j = 0, (i \neq j)$.

C_{P_d} : A constant representing the ratio of the maximum values δ_{imax} and the standard deviations σ_i.

Let us consider a case of the plane feature shown in Fig. 1 (a), as an example. The maximum values δ_{imax} are given in the followings.

$$\delta_1 = w, \delta_2 = \alpha, \delta_3 = \beta$$

$$\delta_{1max} = \frac{t}{2}, \delta_{2max} = \frac{t}{L_1}, \delta_{3max} = \frac{t}{L_2} \quad (2)$$

where,

L_1, L_2 : Length and width of the plane feature.

t : Tolerance values, e.g. the distance between two planes representing the tolerance zones.

From Eqs. (1) and (2), the standard deviation of three deviation parameters are given in the followings.

$$\sigma_1 = \frac{t}{2C_{Pd}}, \sigma_2 = \frac{t}{L_1 C_{Pd}}, \sigma_3 = \frac{t}{LC_{Pd}} \quad (3)$$

The following equation gives the conditions that the plane features are included within the tolerance zone between a pair of planes.

$$-\frac{t}{2} \leq \delta_1 + \frac{L_1\delta_2}{2} + \frac{L_2\delta_3}{2} \leq \frac{t}{2} \quad (4)$$

The probability that the toleranced features are included within the tolerance zone is given by the following equation. This probability $1 - P_d$ means the non-defective rate.

$$1 - P_d = \left(\frac{2}{\sqrt{2\pi}}\right)^3 \int_0^{C_{Pd}} \int_0^{C_{Pd}-x_1} \int_0^{C_{Pd}-x_1-x_2} \left(\prod_{i=1}^{3} \exp\left(-\frac{x_i^2}{2}\right)\right) dx_3 dx_2 dx_1 \quad (5)$$

where,

$$x_1 = \frac{2C_{P_d}\delta_1}{t}, x_2 = \frac{L_1 C_{P_d}\delta_2}{t}, x_3 = \frac{L_2 C_{P_d}\delta_3}{t}$$

If the defective rate P_d is set to 0.27%, the constant C_{Pd} can be estimated as "C_{Pd} = 5.83", through the numerical analysis of Eq. (5).

In the case of a cylinder shown in Fig. 1 (b), the following equation gives the standard deviations of the parameters.

$$\delta_1 = u\ \delta_2 = w, \delta_3 = \alpha, \delta_4 = \gamma$$
$$\delta_{1max}, \delta_{2max} = \frac{t}{2}, \delta_{3max}, \delta_{4max} = \frac{t}{L} \quad (6)$$
$$\sigma_1, \sigma_2 = \frac{t}{2C_{Pd}}, \sigma_3, \sigma_4 = \frac{t}{LC_{Pd}}$$

In this case, the C_{P_d} is estimated as "C_{P_d}= 5.06," for the case that the defective rate P_d is 0.27%.

In the case of the sphere shown in Fig.1 (c), the following equation gives the standard deviations of the parameters.

$$\delta_1 = u, \delta_2 = v, \delta_3 = w$$
$$\delta_{1max}, \delta_{2max}, \delta_{3max} = \frac{t}{2}, \sigma_1, \sigma_2, \sigma_3 = \frac{t}{2C_{Pd}} \quad (7)$$

In this case, the C_{P_d} is estimated as "C_{P_d}=3.57", for the case that the defective rate P_d is set to be 0.27%.

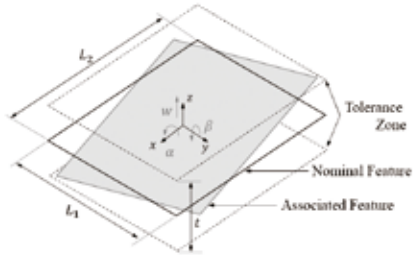

(a) Plane feature

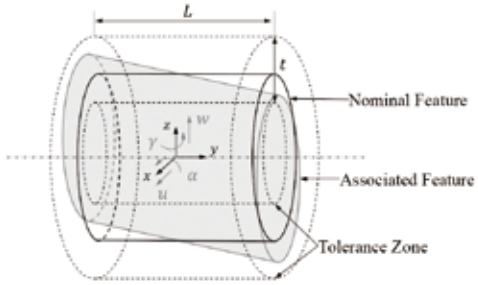

(b) Cylinder feature

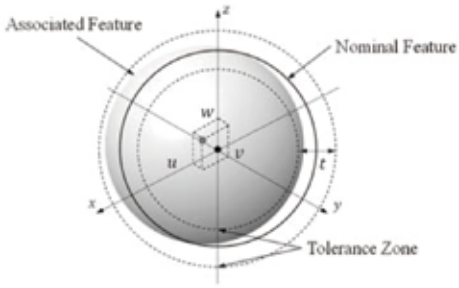

(c) Sphere Feature

Fig. 1 Definition of geometric tolerance of features

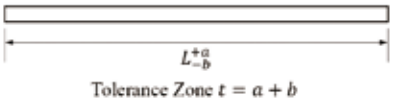

Fig. 2 Tolerance zone of dimensional tolerances

As regards to the dimensional tolerances of the link lengths, the tolerance zones are represented by the value $t = a + b$ as shown in Fig. 2, and the value t represent the ranges of $\pm 3\sigma$. Therefore, the following equation gives the standard deviation of the parameters. In this case, "C_{P_d}= 3", for the case that the defective rate P_d is set to be 0.27%.

$$\delta_{max} = \frac{t}{2}, \sigma = \frac{t}{2C_{P_d}} \tag{8}$$

3. Modeling and Analysis of Parallel Link Robots

3.1 Parallel link robot system description

The parallel link robots considered in the research are shown in Figs 3 and 4, which represent the 3-dimensional model and the kinematic model, respectively. The end-effectors move in the 3-dimensional space against the fixed bases. The motions of the end-effectors are limited to the parallel motions with three degree of freedom. The motions are controlled by the rotational angles θ_1, θ_2 and θ_3 of the upper links in the kinematic model shown in Fig. 4.

Three servo-motors are equipped within the bases to independently control the rotational angles θ_1, θ_2 and θ_3 of the upper links. The lower links shown in Fig. 4 are connected by two double spherical joints with the upper links in one end and with the end-effectors in the opposite end. By connecting with use of the double spherical joints, the motions of the end-effectors are limited to the parallel motions without rotations.

Figure 5 summarizes the geometric parameters representing the link lengths and the positions of the joints which connect the bases, the upper links, the lower links and the end-effectors.

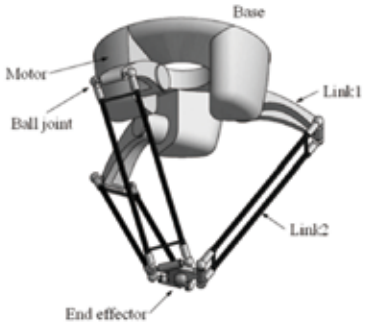

Fig. 3 Parallel link robot

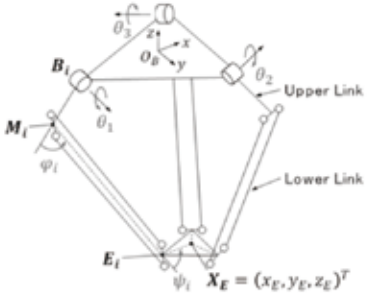

Fig. 4 Kinematic diagram

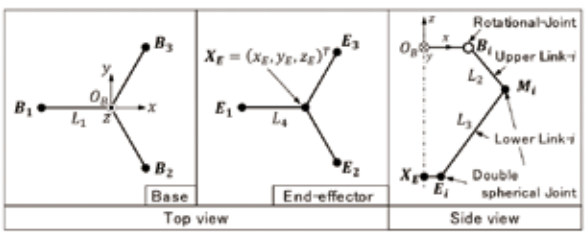

Fig. 5 Kinematic parameters

3.2 Inverse kinematics analysis

Denavit Hartenberg has proposed the D-H method, which is commonly applied to the robot kinematic models. In the research, inverse kinematics analysis is considered to determine the active link position angle $\theta_i (i=1,2,3)$ based on the position (x_E, y_E, z_E) of the moving end-effectors.

The inverse kinematic analysis is required to determine the joint angles θ_1, θ_2 and θ_3 of the upper links based on the position of the end-effectors. This section deals with the method to determine these joint angles.

The input information about the position of the end-effector is given by a position vectors $\boldsymbol{X_E}$ representing the center positions of the end-effectors.

$$\boldsymbol{X_E} = (x_E, y_E, z_E)^T \tag{9}$$

Equation (10) gives the basic conditions to determine the joint angles θ_1, θ_2 and θ_3 based on $\boldsymbol{X_E}$.

$$L_3^2 = |\boldsymbol{E_i} - \boldsymbol{M_i}|^2 \quad (i = 1,2,3) \tag{10}$$

The $\boldsymbol{M_i}$ and $\boldsymbol{E_i}$ are given by Eqs. (11) and (12), according to the kinematic diagram shown in Fig. 4.

$$\begin{aligned}
\boldsymbol{M_1} &= \begin{Bmatrix} L_1 + L_2\cos\theta_1 \\ 0 \\ -L_2\sin\theta_1 \end{Bmatrix} \\
\boldsymbol{M_2} &= \begin{Bmatrix} \frac{1}{2}L_1 - \frac{1}{2}L_2\cos\theta_2, \\ \frac{\sqrt{3}}{2}L_1 + \frac{\sqrt{3}}{2}L_2\cos\theta_2 \\ -L_2\sin\theta_2 \end{Bmatrix} \\
\boldsymbol{M_3} &= \begin{Bmatrix} \frac{1}{2}L_1 - \frac{1}{2}L_2\cos\theta_3, \\ \frac{\sqrt{3}}{2}L_1 - \frac{\sqrt{3}}{2}L_2\cos\theta_3 \\ -L_2\sin\theta_3 \end{Bmatrix}
\end{aligned} \tag{11}$$

$$\begin{aligned}
\boldsymbol{E_1} &= \{+L_4, y_E, z_E\} \\
\boldsymbol{E_2} &= \left\{x_E - \frac{L_4}{2}, y_E + \frac{\sqrt{3}}{2}L_4, z_E\right\} \\
\boldsymbol{E_3} &= \left\{x_E - \frac{L_4}{2}, y_E - \frac{\sqrt{3}}{2}L_4, z_E\right\}
\end{aligned} \tag{12}$$

Three independent equations shown in Eq. (13) are obtained based on the Eqs. (9) to (12).

$$A_i\cos\theta_i + B_i\sin\theta_i = C_i \tag{13}$$

where,

$$A_1 = x + L_4 - L_1, B_1 = z, C_1 = \frac{L_3^2 - L_2^2 - A_1^2 - y^2 - z^2}{2L_2}$$

$$A_2 = \frac{1}{2}\left(D_2 + \sqrt{3}E_2\right), B_2 = z, C_2 = \frac{L_3^2 - L_2^2 - D_2^2 - E_2^2 - z^2}{2L_2}$$

$$D_2 = x - \frac{1}{2}L_4 + \frac{1}{2}L_1, \quad E_2 = y + \frac{\sqrt{3}}{2}L_4 - \frac{\sqrt{3}}{2}L_1$$

$$A_3 = \frac{1}{2}\left(D_3 + \sqrt{3}E_3\right), B_3 = z, C_3 = \frac{L_3^2 - L_2^2 - D_3^2 - E_3^2 - z^2}{2L_2}$$

$$D_3 = x - \frac{1}{2}L_4 + \frac{1}{2}L_1, \quad E_3 = y + \frac{\sqrt{3}}{2}L_4 + \frac{\sqrt{3}}{2}L_1$$

The joint angles θ_i are finally obtained by the following equations.

$$\theta_i = -\tan^{-1}(B_i, A_i) - \tan^{-1}\left(C_i, \sqrt{A_i^2 + B_i^2 - C_i^2}\right) \quad (14)$$

The angles φ_i and ψ_i shown in Fig. 4 are obtained by the following equations. These angles are required to estimate the position of the end-effectors taking into consideration of the geometric deviations of both the joints and the link lengths.

$$\varphi_i = \cos^{-1}\left(\frac{\boldsymbol{M_iB_i}\cdot\boldsymbol{M_iE_i}}{|\boldsymbol{M_iB_i}||\boldsymbol{M_iE_i}|}\right)$$
$$\psi_i = \cos^{-1}\left(\frac{\boldsymbol{E_iM_i}\cdot\boldsymbol{E_iX_E}}{|\boldsymbol{E_iM_i}||\boldsymbol{E_iX_E}|}\right) \quad (15)$$

4. Modeling of Parallel Link Robots

4.1 Kinematic motion deviations of rotational joints

The parallel link robots shown in Figs. 4 and 5 have two types of joints. They are the rotational joints between the base and the upper kinks and the spherical joints between the other links. 4 by 4 homogeneous transformation matrices are applied to represent the kinematic motions in the paper. The kinematic motions at the rotational joints shown in Fig. 6 are represented by the following equation taking into consideration of the geometric deviations of the faces. The standard deviations of parameters $\delta\alpha, \delta\gamma, \delta x, \delta y, \delta z$ are calculated by applying Eqs. (3) to (6) in the following equation.

$$A_5^{\sigma}(\theta) = \begin{pmatrix} \cos\theta & \delta\gamma_{\theta 1} & \sin\theta & \delta x_\theta \\ \delta\gamma_{\theta 2} & 1 & \delta\alpha_{\theta 1} & \delta y_\theta \\ -\sin\theta & \delta\alpha_{\theta 2} & \cos\theta & \delta z_\theta \\ 0 & 0 & 0 & 1 \end{pmatrix} \quad (16)$$

where,
$\delta\alpha_{\theta 1} = \gamma_{ia}\sin\theta - \alpha_{ia}\cos\theta + \alpha_{jb}$
$\delta\alpha_{\theta 2} = -\gamma_{jb}\sin\theta - \alpha_{jb}\cos\theta + \alpha_{ia}$
$\delta\gamma_{\theta 1} = \gamma_{jb}\cos\theta - \alpha_{jb}\sin\theta - \gamma_{ia}$,
$\delta\gamma_{\theta 2} = \gamma_{ja}\cos\theta + \alpha_{ja}\sin\theta - \gamma_{jb}$
$\delta x_\theta = \frac{1}{2}\left(-2\delta x_{jb} + l_1\gamma_{jb} + l_4\gamma_{jb}\right)\cos\theta - (l_1 + l_4)\gamma_{ia} - \frac{1}{2}\left(2\delta z_{jb} + l_1\alpha_{jb} + l_4\alpha_{jb}\right)\sin\theta + \delta x_{ia}$
$\delta y_\theta = \delta y_{ic} - \delta y_{jc}$
$\delta z_\theta = \frac{1}{2}\left(-2\delta x_{jb} + l_1\gamma_{jb} + l_4\gamma_{jb}\right)\sin\theta + (l_1 + l_4)\alpha_{ia} - \frac{1}{2}\left(2\delta z_{jb} + l_1\alpha_{jb} + l_4\alpha_{jb}\right)\cos\theta + \delta z_{ia}$
α_{mn}, γ_{mn} : Orientation deviations of guide-way n in Unit-m $(m = i, j, n = a, b)$
$\delta x_{mn}, \delta y_{mn}, \delta z_{mn}$: Position deviations of guide-way n in Unit-m $(m = i, j, n = a, b)$

4.2 Kinematic motion deviations of spherical joints

The kinematic motions in the spherical joints shown in Fig.7 are represented by only the angles of φ_i or ψ_i, as shown in Fig. 4, and the transformation matrix for the spherical joints with geometric deviations is given by the following equations.

$$A_6^{\sigma}(\varphi) = \begin{pmatrix} \cos\varphi & -\sin\varphi & 0 & \delta x_\varphi \\ \sin\varphi & \cos\varphi & 0 & \delta y_\varphi \\ 0 & 0 & 1 & \delta z_\varphi \\ 0 & 0 & 0 & 1 \end{pmatrix} \quad (17)$$

where,
$\delta x_\varphi = -\delta x_d\cos\varphi + \delta y_d\sin\varphi + \delta x_e$,
$\delta y_\varphi = -\delta x_d\sin\varphi - \delta y_d\cos\varphi + \delta y_e$,
$\delta z_\varphi = \delta z_e - \delta z_d$
$\delta x_n, \delta y_n, \delta z_n$: Position deviations of joint n

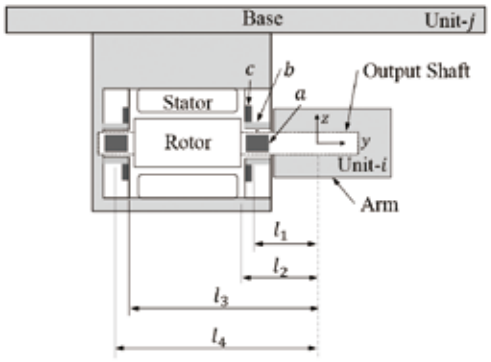

Fig. 6 Rrotational joints with motors

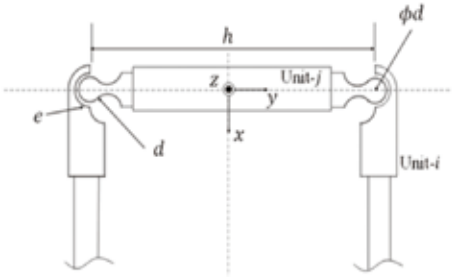

Fig. 7 Spherical joints

4.3 Modeling of kinematic motions of parallel link robots

The positions $\boldsymbol{E_i}$ in Eq. (12) are given in the following Eq. (18), and the positions $\boldsymbol{X_E}$ of the centers of the end-effectors are obtained as the center of three points of the $\boldsymbol{E_1}, \boldsymbol{E_2}, \boldsymbol{E_3}$.

$$\boldsymbol{E_i} = A_1(L_1)A_5^{\sigma}(\theta)A_1(L_2)A_4(\alpha_i)A_6^{\sigma}(\pi - \varphi_i)A_1(L_3)A_4(\beta_i)A_6^{\sigma}(\pi - \psi_i) \quad (18)$$

where,
$A_1(L_i)$: Translation between the coordinates system
$A^4(\alpha_i, \beta_i)$: Rotation between the coordinates system
$A^5(\theta)$: Rotation of the motors
$A^6(\pi - \varphi_i, \pi - \psi_i)$: Rotation of the spherical joints

The kinematic motion deviations of the centers of the end-effectors are obtained as the standard deviations of the

position vectors $\boldsymbol{X_E}$ in the x, y and z directions, and represented by the following equations.

$$\sigma_{X_E} = (\sigma_x, \sigma_y, \sigma_z)$$

$$\sigma_x = \frac{1}{3}\sqrt{\sigma_{x_1}^2 + \sigma_{x_2}^2 + \sigma_{x_3}^2}$$
$$\sigma_y = \frac{1}{3}\sqrt{\sigma_{y_1}^2 + \sigma_{y_2}^2 + \sigma_{y_3}^2} \quad (19)$$

$$\sigma_z = \frac{1}{3}\sqrt{\sigma_{z_1}^2 + \sigma_{z_2}^2 + \sigma_{z_3}^2}$$

where,

$\sigma_{xi}, \sigma_{yi}, \sigma_{zi}$: Standard deviations of the position vectors $\boldsymbol{E}_i$ in x, y and z directions.

5. Tolerance Design

The tolerance design of the parallel link robots plays an important role from the viewpoints of both the kinematic motion accuracy and the production costs. The tolerance values should be as large as possible for the ease of manufacturing processes. On the other hands, the end-effectors of the parallel link robots should be controlled so that their kinematic motion deviations are kept within the allowable ranges.

A systematic procedure is proposed here, by applying an optimization method, to determine a suitable set of the tolerance values of all the joints and the links under the constraints on the kinematic motion deviations of the centers of the end-effectors. The tolerance design problem considered here is formulated as shown in the followings, in order to consider the trade-off between the high kinematic motion accuracy and the ease of the manufacturing processes.

The design variables summarized in Table 1 include five geometric tolerance values from t_1 to t_5 of the joints shown in Figs. 3 and 4, and two-dimensional tolerance values t_6 and t_7 of the upper links and the lower links shown in Fig. 4.

The following equation gives the objective function including the tolerance values and the representative dimensions of the grometric elements of the joints and the links.

$$\min \; g = \sum_{i=1}^{7} \frac{r_i^{0.34}}{t_i} \quad (20)$$

where, r_i is the representative dimensions of the components.

The objective function Eq. (20) is formulated on the basis of the relations between the tolerance values and the representative dimentions of the featrures defined in the IT standard tolerance

The following Equation gives the constraints on the kinematic motion deviations of the end-effectors estimated by the equations from (16) to (19).

$$f \le f_{max}, \; f = \sqrt{\sigma_x^2 + \sigma_y^2 + \sigma_z^2} \quad (21)$$

where, f_{max} is the allowable range of the standard deviation of the kinematic motion deviations of the end-effectors, and σ_i is standard deviations in i-direction of the position X_E.

Table 1 Design variables for seven kinds of tolerances

Symbol	Meaning	Guide-way
t_1	Radial axis	a
t_2	Radial bearing	b
t_3	Thrust bearing	c
t_4	Spherical joints (Ball)	d
t_5	Spherical joints (Socket)	e
t_6	Dimensional tolerance of upper link	
t_7	Dimensional tolerance of lower link	

6. Case Study

The proposed method is applied to the tolerance design of the parallel link robot shown in Fig. 3 by setting the allowable kinematic deviation to 0.05 mm. Figure 8 shows the optimum solutions.

The designed tolerance values of t_1, t_2 are smaller than other tolerance values, as shown in Fig. 8. This means that the kinematic motion deviations of the end-effectors is deeply influenced by the tolerance values of the rotational joints between the base and the upper links. Therefore, the tolerance values are rather important to reduce the standard deviations of kinematic motion deviations of the end-effectors.

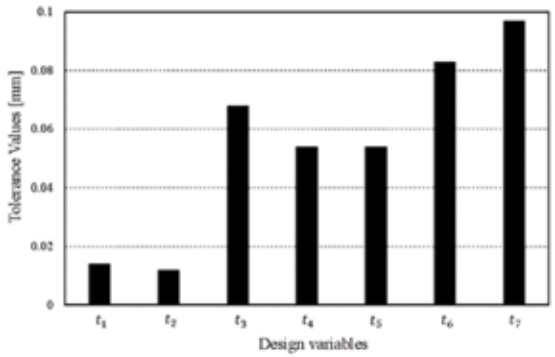

Fig. 8 The result of tolerance design values

7. Experiments and Comparison with Machine Tools

The kinematic motion deviations of a parallel link robot are measured by applying the DBB (Double Ball Bar) system, as shown in Fig. 9, in order to verify the theoretical analysis presented in the paper, and the measured results are compared with the simulation results. The kinematic motion deviations of the parallel link robots are also compared with the ones of the machine tools.

The robot and the measuring system applied are FANUC M-1iA/1H and Renishaw BC20-W, respectively. The terminals of the DBB are fixed on both the table center and the end-effector, and the end-effector is controlled to rotate around the table center. The rotational radius and the feed speed are set to 100 mm and 1,200 mm/sec, respectively. An example of the measurement results is shown in Fig. 10 (a) representing the radial position deviations of the end-effector. As shown in the figure, the trajectory of the end-effector has an ellipsoidal shape, and the radial positioning deviations reach about 0.8 mm.

A mathematical simulation method is also applied to estimation of the effects of the deviations in the lengths of the links constituting the parallel link robots and the alignment deviations of the rotational joints of the upper links which control the positions of the end effectors. The mathematical

simulations have been carries out for the configurations with various link lengths and rotational joint positions of the robot shown in Figs. 3 to 5. One set of the rotational joint, the upper link and the lower link in $-x$ direction in Figs. 4 and 5 are selected, and the position the joint and the lengths of the links are changed in the simulation. The parameters changed in the simulations are the position of the rotational joint L_1, the length L_2 of the upper link and the length L_3 of the lower link in Fig. 5.

The nominal values of L_1, L_2 and L_3 are 110 mm, 100mm and 270 mm, respectively. In the simulation, these parameters are changed in the range of ±1.1 mm. One example of the trajectories obtained in the simulation is shown in Fig. 10 (b) under the conditions of L_1=110 - 1.1, L_2=100 + 1.0 and L_3 =270 - 1.0. The trajectory obtained here has a similar pattern with the trajectory shown in Fig. 10 (a) obtained in the experiments.

The results obtained through both the experiments and the simulations show that it is important to design the geometric deviations of the link lengths and the alignment deviations of the rotational joints from the viewpoint of improving the kinematic motion deviations of the end-effectors.

Figure 11 shows examples of measurement results of kinematic motion deviations of a typical machining center and a portable NC milling machine. The figures show that the kinematic motion deviations of the machining center and the portable milling machines are about 8 μm and 100 μm, respectively. The machining center and the portable milling machine are equipped with the semi-closed loop servo system and the open loop servo system, and the motion deviations the machining center is about ten times smaller than ones of the portable NC milling machine.

The parallel link robot is also equipped with open loop servo system, however the kinematic motion deviations are about 10 times larger than the portable NC milling machines. It is because that the geometric deviations of the link lengths and the alignment deviations of the rotational joints affect the increase of the kinematic motion deviations of the end-effectors.

8. Conclusion

A systematic method is proposed, by applying an optimization method, to determine a suitable set of the tolerance values of the geometric elements of the joints and the links constituting the parallel link robots, under the constraints on the kinematic motion deviations of the end effectors. The results are summarized as follows;

(1) A mathematical model of the parallel link robots was proposed to estimate the kinematic motion deviations of the robots based on the goemetric deviations of the joints and the links. The inverse kinematic method was also discussed to obtain the joint angles of the upper links to control the end-effectors, based on the nominal model without the geometric deviations.

(2) A tolerance design method was proposed and applied to a design problem of the parallel link robots to design a suitable set of the tolerance values of the geometric elements of the joints and the links. The method provides us with a systematic method to determine the suitable set of the tolerance values taking into consideration of both the constraints of the kinematic motion deviations of the end-effectors and the ease of the manufacturing process of the robots and their components.

(3) Kinematic motion deviations of a parallel link robot were measured and compared with the simulation results based on the kinematic model. The results show that the kinematic motion deviations of the end-effectors of the robot are deeply affected by the geometric tolerances of the joints and the links constituting the robots. The kinematic motion deviations of the machining center and the portable NC milling machine were measured, and compared with the ones of the parallel link robot to verify the motion accuracy of the robots.

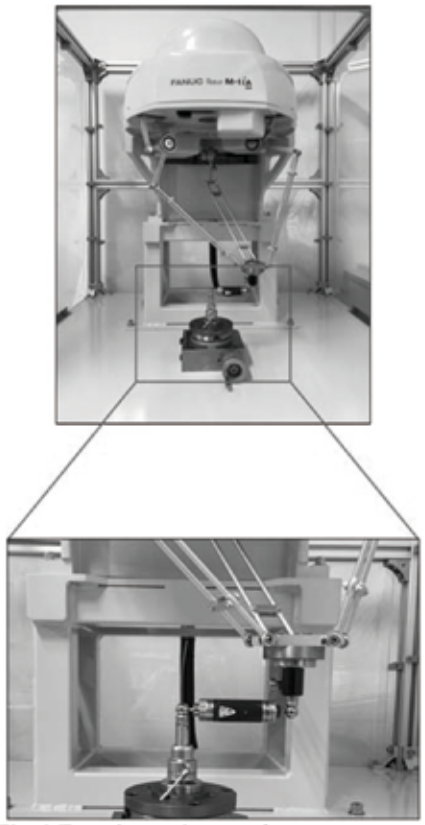

Fig. 9 Experimental set-up for measurements

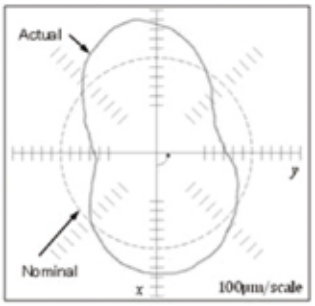

(a) Experimental result

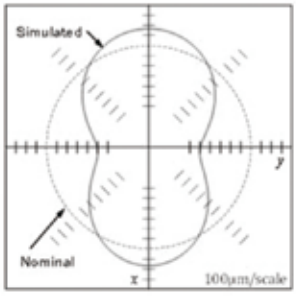

(b) Simulation result

Fig. 10 Measurement and simulation results of kinematic motion deviations of parallel link robot

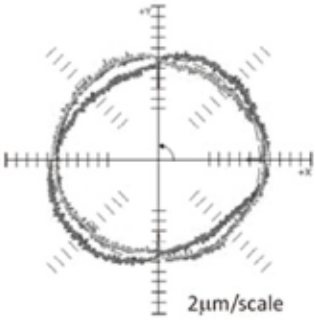

(a) Machining center

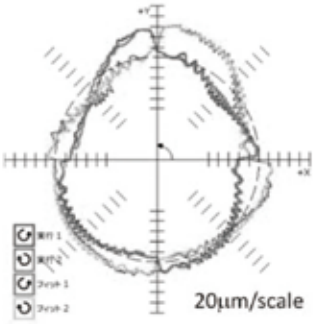

(b) Portable NC milling machine

Fig. 11 Measured kinematic motion deviations of machine tools

Acknowledgements

The measurement experiments were carried out in the manufacturing system laboratory at Osaka Prefecture University. The author would like to express his sincere appreciations to Prof. Koji Iwamura at Osaka Prefecture University for his corporation and supports in the research.

References

[1] Carrino, L., Moroni, G., Polini, W. and Semeraro, W.: 3D Tolerance analysis involving geometric tolerances, paper presented in the 34th CIRP International Seminar of Manufacturing Systems, Athens, Greece, 29-38, 2001.

[2] Mathieu, L., Clement, A. and Bourdet, P.: Modelling, representation, processing and inspection of tolerances: A survey, paper presented in the 5th CIRP Seminar on Computer Aided Tolerancing, Toronto, Canada, 1-38, 1997.

[3] Narahari, Y., Sudarson, R., Lyous, K., Duffy, M. R. and Sriran, R. D.: Design for tolerance of electro-mechanical assemblies: An integrated approach, IEEE Transactions on Robotics and Automation, vol. 15(6), 1062-1079, 1999.

[4] Ngoi, B. K. A. and Agarwal, M.: The generic capsule approach to tolerance stack analysis, International Journal of Production Research, 36(12), 3273-3293, 1998.

[5] Ngoi, B. K. A., Lim, B. H. and Ang, P. S.: Nexus method for stack analysis of geometric dimensioning and tolerancing (GDT) problems, International Journal of Production Research, 38(1), 21-37, 2000.

[6] Roy, U., Liu, C. R. and Woo T. C.: A review of dimensioning and tolerancing: Representation and processing, Computer-Aided Design, 23(7), 466-483, 1991.

[7] Satonaka, N., Sugimura, N., Tanimizu, Y. and Iwamura, K.: A study on modeling and analysis of kinematic motion deviations of machine tools (1st Report, Modeling and analysis of geometric deviations of constituting units), Transactions of the JSME, Series C, 71(708), 192-198, 2005 (in Japanese).

[8] Satonaka, N., Sugimura, N., Tanimizu, Y. and Iwamura, K.: Analysis of geometric deviations of machine products under Maximum Material Conditions, Transactions of the JSME, Series C, 73(730), 285-291, 2007 (in Japanese).

[9] Satonaka, N., Sugimura, N., Tanimizu, Y. and Iwamura, K.: A study on modeling and analysis of kinematic motion deviations of machine tools (2nd Report, Modeling and Analysis of Linear Tables and Machine Tools), Transactions of the JSME, Series C, 74(737), 198-205, 2008 (in Japanese).

[10] Sugimura, N., Watabiki, H., Thasana, W., Iwamura, K. and Tanimizu, Y.: Analysis of Kinematic Motion Deviations of Rotary Tables Based on Geometric Tolerances, Journal of Advanced Mechanical Design, Systems, and Manufacturing, JSME, 6(7), 1132-1142, 2012.

[11] Takahashi, A., Yoshida, A., Thasana, W., Sugimura, N., Iwamura, K. and Tanimizu, Y. (2014). Analysis of Kinematic Motion Deviations of Machining Centers Based on Geometric Tolerances, Journal of Advanced Mechanical Design, Systems, and Manufacturing, JSME, 8(4), 1-12, 2014.

[12] Takematsu, R., Sugimura, N., Yoshida, A., Thasana, W., Tanimizu, Y. and Iwamura, K.: A Study on Tolerance Design for Machine Tools based on Shape Generation Functions, The 6th TSME International Conference on Mechanical Engineering (the 6th TSME-ICoME 2015), Hua-Hin, Thailand, 2015.

[13] Tsumura, T. and Ohnishi, K.: Machine Design and Drawing Handbook based on JIS, Rikogakusya Co. Ltd., pp. 17-85, 2001 (in Japanese).